Articles

Increased Backbone Flexibility in Threonine[45]-Phosphorylated Hirudin upon pH Change[†]

Marc Kipping, Toralf Zarnt, Steffen Kiessig, Ulf Reimer, Gunter Fischer,* and Peter Bayer[‡]

Max Planck Research Unit for Enzymology of Protein Folding, Weinbergweg 22, 06120 Halle, Germany

Received February 14, 2001; Revised Manuscript Received May 1, 2001

ABSTRACT: Protein phosphorylation on serine/threonine side chains represents a major regulatory event in the posttranslational control of protein functionality, where it is thought to operate at the level of structural changes in the polypeptide chain. However, key questions about molecular aspects of phosphate ester induced conformational alterations remain open. Among these concerns are the radius of action of the phosphate ester group, its effective ionic state, and its interplay with distinct bonds of the polypeptide chain. Primarily to define short-range effects upon threonine phosphorylation, the native 65 amino acid protein hirudin, conformationally restrained by a proline flanking the pThr[45] site and three intramolecular disulfide bonds, was structurally characterized in both the phosphorylated and the unphosphorylated state in solution. Circular dichroism and hydrogen exchange experiments (MALDI-TOF) showed that structural changes were caused by Thr[45]-Pro[46] phosphorylation only when the phosphate ester group was in its dianionic state. The spatial arrangement of the amino acids, monitored by ^{1}H NMR spectroscopy, appears to be affected within a radius of about 10 Å around the pThr[45]-OγH, with phosphorylation resulting in a loss of structure and increased flexibility within a segment of at least seven amino acid residues. Thus, the transition from the monoanionic to the dianionic phosphate group over the pH range 5.2−8.5 represents a general phosphorylation-dependent conformational switch operating at physiological pH values.

The cascade of phosphorylation and dephosphorylation at serine and threonine side chains of proteins is one of the most common bases for the reversible control of protein activity. Protein Ser/Thr kinases and phosphatases catalyze this type of posttranslational modification (reviewed in refs *1*, *7*, and *12*). In addition to steric blockage of the active site, as in the case of isocitrate dehydrogenase (*11*), Ser/Thr phosphorylation may also cause major conformational alterations in the protein structure. Two prominent examples of long-range conformational rearrangements induced by phosphorylation are provided by (1) glycogen phosphorylase (*19*), which has been crystallized in the active phosphorylated and the inactive nonphosphorylated form, and (2) the bacterial NTRc protein determined by nuclear magnetic resonance studies (*15*). It is thought that attractive or repulsive forces introduced by the phosphate ester group play the major role in chain displacement. In addition, phosphorylation-induced conformational changes are thought to be responsible for the altered thermodynamic stability of several proteins. These include protein kinase C$_\alpha$ (*2*) and phytochrome A (*17*). A helix-dipole stabilizing effect has been reported for the phosphorylation of the HPr protein (*23*), and a perturbation of secondary structure by phosphorylation was observed for the cytoplasmic domain of phospholambam (*18*, *21*). Phosphorylation also seems to affect the morphology of bacterial fibers of *Neisseria gonorrheae*, which are responsible for the virulent attachment and motility of numerous bacterial pathogens (*6*).

Despite such numerous studies, there is a lack of information about fundamental molecular aspects of the phosphate ester effects, including the influence of the protonation state of the phosphate ester group, and the radial extension of its effects into neighboring polypeptide segments. Conformational changes in short model peptides, which were recently observed upon phosphorylation of a Ser/Thr site (*26*, *29*), shed some light on how a pH-sensitive structural rearrangement induced by protein phosphorylation may function on the peptide level.

The present work compares the pH-dependent conformational states of hirudin in its phosphorylated form with those in its nonphosphorylated form. Residue Thr[45] of the Thr[45]-Pro[46] moiety was identified as the phosphorylated amino acid (*4*). Thr[45] is located on the surface of hirudin (Figure 1) and is revealed by its signature sequence as an accessible target site for proline-directed protein kinases (*3*, *16*). The phosphate ester moiety of pThr[45] is located greatly distant from

[†] P.B. was supported by DFG Grant Ba1624/3-1.

* Corresponding author: fax, +49 345 551 1972; phone, +49 345 55 22801; e-mail, fischer@enzyme-halle.mpg.de.

[‡] Current address: Max Planck Institute for Molecular Physiology, Junior Research Group "Molecular and Structural Biophysics", Otto-Hahn Strasse 11, 44227 Dortmund, Germany.

10.1021/bi010317r CCC: $20.00
Published on Web 06/15/2001

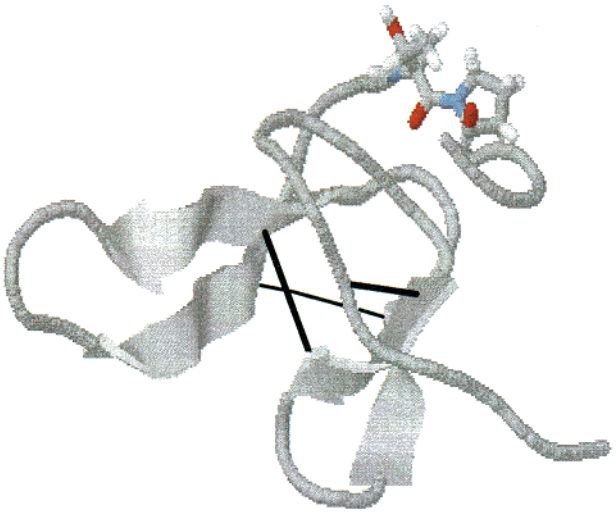

FIGURE 1: Top: Schematic drawing of the backbone conformation of hirudin (variant 1) N-terminal core domain 1−51 (*28*) using the program RasMol, v. 2.6 (*25*), and the PDB file 1HIC. Positions of Thr[45] and Pro[46] are indicated by sticks. The three disulfide bonds are symbolized by lines. Bottom: Amino acid sequence of hirudin used in this paper. Merely, the two N-terminal amino acids (Leu-Thr-) differ from the natural sequence of hirudin (variant 1) (Val-Val-). Plain lines and asterisk represent disulfide bridges and the phosphorylated threonine residue, respectively.

charged residues (>5.3 Å). Such a distance, taken together with the rigid hirudin structure, excludes chain rearrangement by formation of short-range salt bridges or charge repulsion. However, conformational changes around the pThr−Pro peptide bond remain a possible mechanism for phosphorylation-induced structural alterations. Therefore, hirudin was chosen as a model system to study influences of phosphorylation upon the local structure of proteins.

MATERIALS AND METHODS

Materials. Recombinant desulfated hirudin and pThr[45]-hirudin[1] were generous gifts from Dr. R. Obermeier (Hoechst AG, Frankfurt, Germany). For further use pThr[45]-hirudin was separated from a yellow pigment in the bulk by gel filtration on a Superdex 75 (16/60) column (Pharmacia, Uppsala, Sweden). PP2A was kindly provided by A. Werner (Halle, Germany). Buffers and all other chemicals were from Sigma (Deisenhofen, Germany) or Serva (Heidelberg, Germany).

Optical Spectroscopy. Protein concentrations were determined spectrophotometrically using the molar extinction coefficients at 280 nm (3280 and 2560 $M^{-1}\cdot cm^{-1}$ for oxidized and reduced hirudin/pThr[45]-hirudin, respectively), which were calculated from the primary structure as described by Gill and von Hippel (*33*). UV/vis spectrometric measurements were performed on a Zeiss Specord S10 diode array UV/vis spectrophotometer.

Far-UV circular dichroism (CD) spectra were measured with a Jasco J710 spectropolarimeter equipped with a thermostated cell holder and a Neslab RTE-100 water-circulating bath in a 0.1 cm cell at 20 °C. At least 16 scans in a range between 250 and 197 nm were averaged for each measurement, and the resulting spectra were normalized to mean residue weight ellipticities and smoothed using the Jasco Series 700 software.

Fluorescence measurements were carried out on a FluoroMax-2 fluorescence spectrometer (Instruments S. A., Edison) in 1 × 1 cm cells. All buffers were filtered to remove insoluble components. All spectra were corrected for the contributions of the buffers and additional sample components by using corresponding references.

NMR Spectroscopy. ^{31}P NMR measurements were performed on a Bruker ARX 500 spectrometer with the proton resonance frequency at 500.13 MHz and the ^{31}P resonance at 202 MHz, respectively. All spectra were recorded at 295 K. Temperature calibration was performed using an 866 thermometer (Keithley). All other spectra were recorded on a Bruker DRX 500 spectrometer equipped with shielded *z*-gradients setting the temperature to 300 K. Calibration was done via a variable temperature unit (Eurotherm B-VT-2000). Samples for pH-dependent measurements contained 5−7 mg of protein dissolved in a H_2O/D_2O (90/10 v/v) mixture. The resulting deuteration ratio of the solvent was 10%. Phosphate spectra were recorded with a broad-band probe head. DSS was used as an internal standard for calibration of the proton resonances. ^{31}P spectra were referenced to 85% phosphoric acid in a spherical container immersed in the sample. The pH of the sample was changed by adding KOH and HCl, respectively. All pH values were measured with a combination glass electrode and not corrected for solvent deuterium isotope effects. The results were fitted to the Henderson−Hasselbalch equation.

Processing, analysis, and visual representation of the 2D spectra were done using the NDEE program package (SpinUp, Dortmund, Germany) on O2 or origin workstations (Silicon Graphics Inc.). Gradient-selected spectra were recorded in the phase-sensitive absorption mode with the TPPI or echo−antiecho−TPPI method. The water resonance was suppressed by applying the WATERGATE sequence (*22*). The time domain data for ^1H frequencies were zero-filled once or twice prior to Fourier transformation. 2D spectra were acquired with 2K data points in the f_2 dimension and 400 data points in the f_1 dimension using 8 or 16 scans. Prior to Fourier transformation all spectra were multiplied with a sine-bell square or sine window function shifted by $\pi/2$ or $\pi/4$.

Hydrogen Exchange Experiments and Mass Spectrometry. Kinetics of deuterium incorporation by exchange of amide protons to deuterons in hirudin and pThr[45]-hirudin was monitored by MALDI-TOF mass spectrometry using a Bruker REFLEX mass spectrometer (Bruker Daltonik GmbH, Germany). The in-exchange of deuterium was initiated by a 10-fold dilution of 140 μM protein buffered with 10 mM ammonium acetate (pH 6.0) in D_2O buffered with 10 mM ammonium acetate (pD 6.0) at 0 °C. In another experiment

[1] Abbreviations: DQF-COSY, double-quantum-filtered correlated spectroscopy; MALDI-TOF-MS, matrix-assisted laser desorption ionization time-of-flight mass spectrometry; NOESY, nuclear Overhauser enhancement spectroscopy; pThr[45]-hirudin, hirudin phosphorylated at Thr[45]; PP2A, protein phosphatase 2A; TOCSY, total correlated spectroscopy.

the hydrogen exchange was started by dilution of the protein buffered with 10 mM ammonium carbonate (pH 8.0) in D_2O buffered with 10 mM ammonium carbonate (pD 8.0) at 0 °C. To stop the incorporation of deuterons at appropriate time points, aqueous quenching buffer was added to the sample, resulting in a final pH of 2.4 and 10% D_2O content. To increase the sensitivity of the method, we developed a new preparation protocol to minimize loss of deuterons during analysis (paper in preparation). Accordingly, the sample preparation and mass spectrometric analysis were performed at −20 °C using a thin-layer preparation technique. At this low temperature a very efficient reduction of the D/H back-exchange has been observed even if the composition of the buffer solution (90% H_2O) favors proton incorporation during sample preparation. In a control experiment the H/D back-exchange of fully deuterated pThr^{45}-hirudin relates to an amount of about 5% of the peptide bond deuterons during sample preparation for mass spectrometry. This value corresponds to the lower limit of back-exchange reported for electrospray ionization mass spectrometry (ESI-MS), which represents the classical method to measure deuteron incorporation (*27*). Data were fitted using Sigma Plot software (Jandel Scientific). Because of the limited number of experimental data points the calculated rate constants must be considered as approximate, whereas the number of exchanging protons has been calculated with a limit of error of about 3%.

RESULTS

Phosphorylation of Thr^{45} of Hirudin Causes pH-Dependent Conformational Changes. Distinct protonation levels of the phosphate ester group have the potential to control the polypeptide backbone structure directly. This is important, as the ability to switch from a singly charged to a doubly charged moiety in a pH range close to neutrality is a unique feature of the phosphate ester group. To study the influence of phosphorylation upon protein conformation, a series of far-UV CD spectra of hirudin and pThr^{45}-hirudin at various pH values (Figure 2) were performed. The very low circular dichroism of both forms of hirudin indicates the regular secondary structural content to be minor, in good agreement with structural data reported by other groups (*5*, *8*, *28*). Nevertheless, the data are clear in indicating the far-UV CD spectrum of hirudin to be independent in the pH range of 5−8. In contrast, the spectrum of pThr^{45}-hirudin is strongly pH dependent, with the pK_a of the phosphorylated form of hirudin calculated from the CD data to be 7.2 (Figure 2 inset). The far-UV CD spectrum of pThr^{45}-hirudin at pH 6.0 (monoanionic phosphate) resembles more closely that of the unmodified hirudin than it does the spectrum of pThr^{45}-hirudin at pH 8.0 (dianionic phosphate). In the spectrum of pThr^{45}-hirudin at pH 8.0 the greater negative CD signal at around 200 nm probably arises from the $\pi-\pi^*$ transitions characteristic of the Cotton effects of peptide bonds (208−210 nm $\pi-\pi^*_{(\parallel)}$, 191−193 nm $\pi-\pi^*_{(\perp)}$). This signal might already indicate a structural change induced by conversion of the phosphate ester group to its dianionic form, but the weak CD signals prevent a definite conclusion about the loss of ordered structure. A pH-induced effect on the preference for particular backbone dihedral angles in phosphorylated oligopeptides, earlier reported by Tholey et al. (*29*), thus

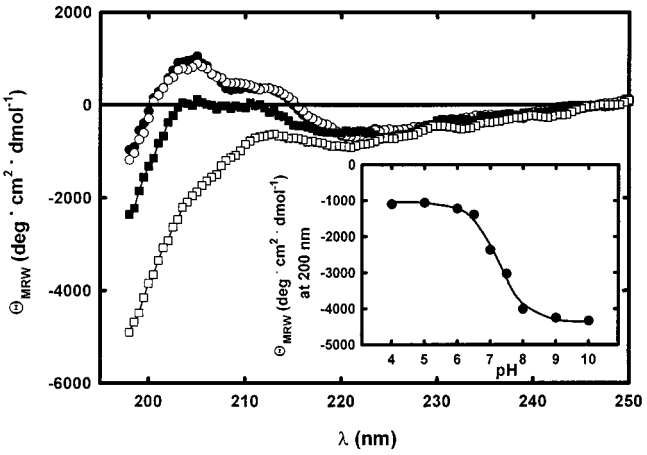

FIGURE 2: Far-UV CD spectra of hirudin at pH 6.0 (●) and pH 8.0 (○) and pThr^{45}-hirudin at pH 6.0 (■) and pH 8.0 (□). The spectra were obtained in 10 mM sodium formate (pH 4.0), 10 mM MES (pH 5.0, 6.0, 6.5), 10 mM sodium phosphate (pH 7.0, 7.5), 10 mM Tris-HCl (pH 8.0, 9.0), and 10 mM sodium borate (pH 10.0) at 20 °C. The protein concentrations were 0.1 mg/mL. The inset shows a titration curve derived from the ellipticities at 200 nm of far-UV CD spectra of pThr^{45}-hirudin at various pHs. The solid line represents the result of a fit according to the Henderson−Hasselbalch relationship (pK_a = 7.2).

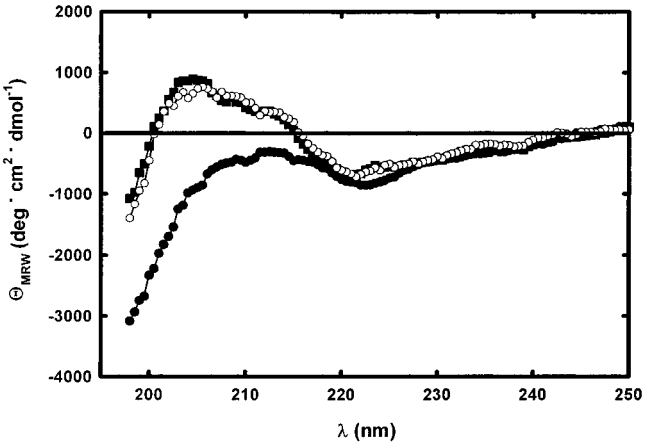

FIGURE 3: Far-UV CD spectra of pThr^{45}-hirudin, before (●) and after (■) PP2A treatment, in comparison with the spectrum of hirudin (○). PP2A (6.4 μM) was incubated with a 20-fold molar excess of pThr^{45}-hirudin for 24 h in 20 mM HEPES (pH 7.5) at 20 °C. The sample was diluted with 10 mM sodium phosphate (pH 7.0), and the far-UV CD spectrum was recorded. The spectra were obtained in 10 mM sodium phosphate (pH 7.0) at 20 °C. The protein concentrations were 0.1 mg/mL.

appears relevant to the backbone dynamics and overall structure of proteins.

The protein kinase responsible for phosphorylation of hirudin is unknown, but the reversibility of the phosphate-based spectral changes was demonstrated by catalyzing dephosphorylation of pThr^{45}-hirudin with protein phosphatase PP2A. The reaction was analyzed by far-UV CD spectroscopy (Figure 3). PP2A had already been shown readily to dephosphorylate the pThr-Pro motif of oligopeptides (*31*). Cleavage of the phosphate ester group on Thr^{45} reestablished the original CD spectrum of hirudin, showing that the secondary structure lacking in pThr^{45}-hirudin is reestablished upon dephosphorylation—a prerequisite for a covalently induced reversible conformational switch. This interpretation of the measured CD spectra is based on the fact that

phosphorylation leads to a spectrum that suggests an increase in random coil, despite the highly constrained structure of hirudin. This is clearly a qualitative result, as it must be, but there is little doubt that phosphorylation produces a rearrangement of chain segments, the details of which will emerge from studies at atomic resolution.

The pThr^{45} Flanking Segment Is Sensitive to Ionization of the Phosphate Ester Group As Probed by ^{1}H NMR. ^{1}H nuclear magnetic resonance spectroscopy directly identifies the amino acid residues affected by the loss of secondary structure upon formation of pThr^{45}-hirudin. The advantages of using NOESY spectra rather than COSY have been discussed by Wang et al. (*30*). Here, NOE cross-peaks in a 2D NOESY spectrum, monitored at different pH values, were used as sensitive probes for conformational changes within particular regions of secondary structure. The pH value was adjusted from 5.2 to 7.9 (hirudin) and 5.2 to 8.5 (pThr^{45}-hirudin), and the differences in both number and strength of NOEs of Thr^{45}-hirudin were recorded at each pH. A clear assignment of NOEs for the amide and aromatic regions was generally possible, but assignments were usually not possible for the aliphatic area, which was densely populated with NOE cross-peaks. As expected from the CD investigations, no change with pH in the number of NOEs was observed for hirudin, although NOE cross-peaks of exchangeable protons broadened as the pH increased. Broadening effects and spectral overlap prevent any conclusions about cross-peak intensity changes. Thus, because of their unreliability, the NOE intensities were not used to deduce structural changes in either hirudin or in pThr^{45}-hirudin. However, close examination of the pThr^{45}-hirudin spectra suggested a pH-induced change in the chemical shifts for several NOEs (Figure 4). To characterize these resonances, homonuclear TOCSY and DQF-COSY spectra for both forms of hirudin were recorded as a function of pH. A pH-dependent chemical shift was observed only for H_N and H_α resonances of amino acids Gly^{42}, Gly^{44}, and Pro^{46}, all near pThr^{45} in pThr^{45}-hirudin. As an example, titration curves of the H_α resonance frequencies of several amino acids are shown in Figure 5A. The *microscopic* "pK_a" (inflection point) values extracted from the C_α proton shifts of pThr^{45}-hirudin lay in the range of 7.3 to 7.6 ($\pm$0.2) and, therefore, are in good agreement with the *macroscopic* pK_a value measured by CD spectroscopy (pK_a = 7.2; Figure 2). Particularly because these shift changes occur only in the phosphorylated form of hirudin and titrate with the same pK_a as the phosphate ester group as monitored by ^{31}P NMR titration studies (pK_a = 6.9 $\pm$ 0.2; Figure 5B), it seems very probable that the structural alterations that give rise to the shift changes are caused by ionization of the phosphate ester group. A movement of all H_α shifts (of more than 0.1 ppm) of protons in the loop region (Gly^{42} to Thr^{45}) in the direction of their random coil values was observed with increasing pH (Figure 6) in the spectra of pThr^{45}-hirudin, showing that the pH-induced rearrangement consists of a loss of ordered structure. In addition to these effects for Gly^{42} to Thr^{45}, similar observations were made for Gln^{11}, and some minor changes (<0.05 ppm) in the H_α chemical shifts were seen for residues Gly^{10}, Asn^{26}, and Pro^{46}. All H_N-H_N and $H_\alpha-H_\alpha$ NOEs that derive from turn and β-sheet elements remained constant during the pH-induced switch. Therefore, the structural rearrangement was a local one, affecting only residues located in the peptide segment preceding the pThr-Pro moiety (i.e., Gly^{42} to Pro^{46}) and their spatial neighboring amino acids (Gln^{11}, Gly^{10}) in the adjacent β-strand. A radius of action of the phosphorylated threonine residue can be defined by measuring the distances between Thr^{45}-OγH and the affected Xaa-H_α. This radius is about 10 Å in the case of pThr^{45}-hirudin.

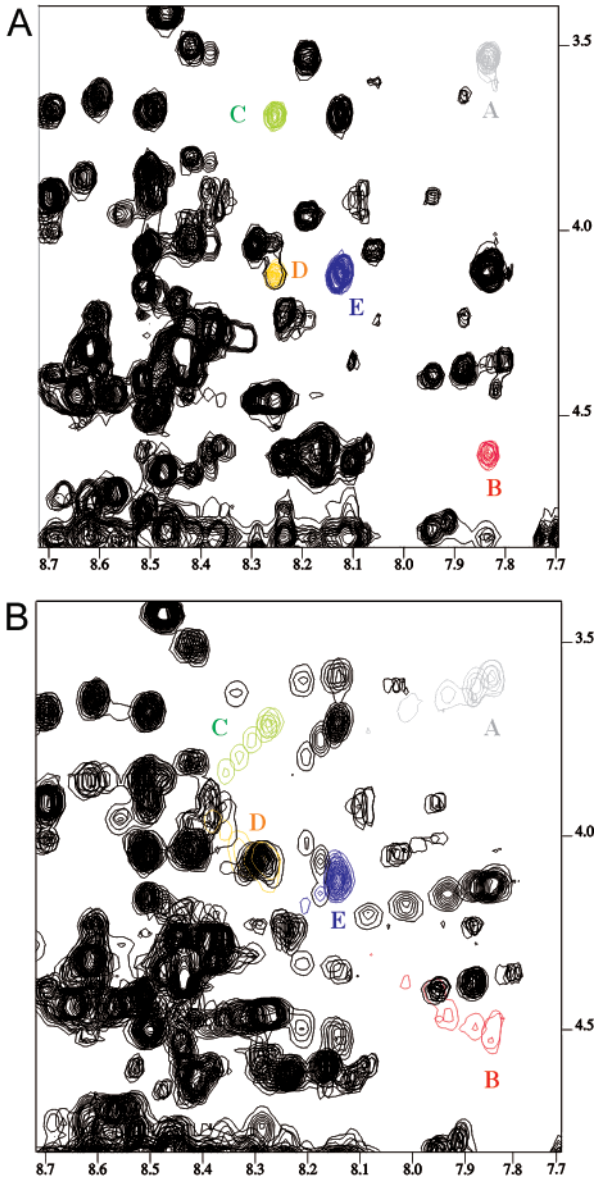

FIGURE 4: (A) Part of the ^{1}H NOESY fingerprint region of hirudin and pThr^{45}-hirudin. $H\alpha_i-HN_i$ NOEs of A (gray) = Gly$^{44}\alpha_1$, B (red) = Gly$^{44}\alpha_2$, C (green) = Gly$^{42}\alpha_1$, D (yellow) = Gly$^{42}\alpha_2$, and E (blue) = Glu^{43} are color-coded. Seven NOESY spectra of hirudin referring to different pH values are superimposed (pH 4.7, 5.2, 5.8, 6.4, 6.9, 7.3, 7.9). (B) Part of the ^{1}H NOESY fingerprint region of pThr^{45}-hirudin. Seven NOESY spectra referring to different pH values are superimposed (pH 5.2, 5.8, 6.4, 6.9, 7.3, 7.9, 8.5). The same color coding as in panel A was used.

H/D Exchange Mass Spectrometry Data Reveal a Loss of Hydrogen Bond Network Dependent on Ionization of pThr^{45}. In previous work on the structural features of hirudin (*8*, *9*), static and transient interactions, mainly involving hydrogen bonds around Thr^{45}, were observed to stabilize the loop and fix the dihedral angles of the surrounding amino acids (Gly$^{42}H_N-$Gly^{25}O, Gly$^{25}H_N-$Glu$^{43}O^\epsilon$, Asn$^{12}H_N-$Thr^{45}O, and possibly Thr$^{45}H_N-$Gly^{10}O). It was possible to explain the chemical shift data on the basis of a perturbed hydrogen

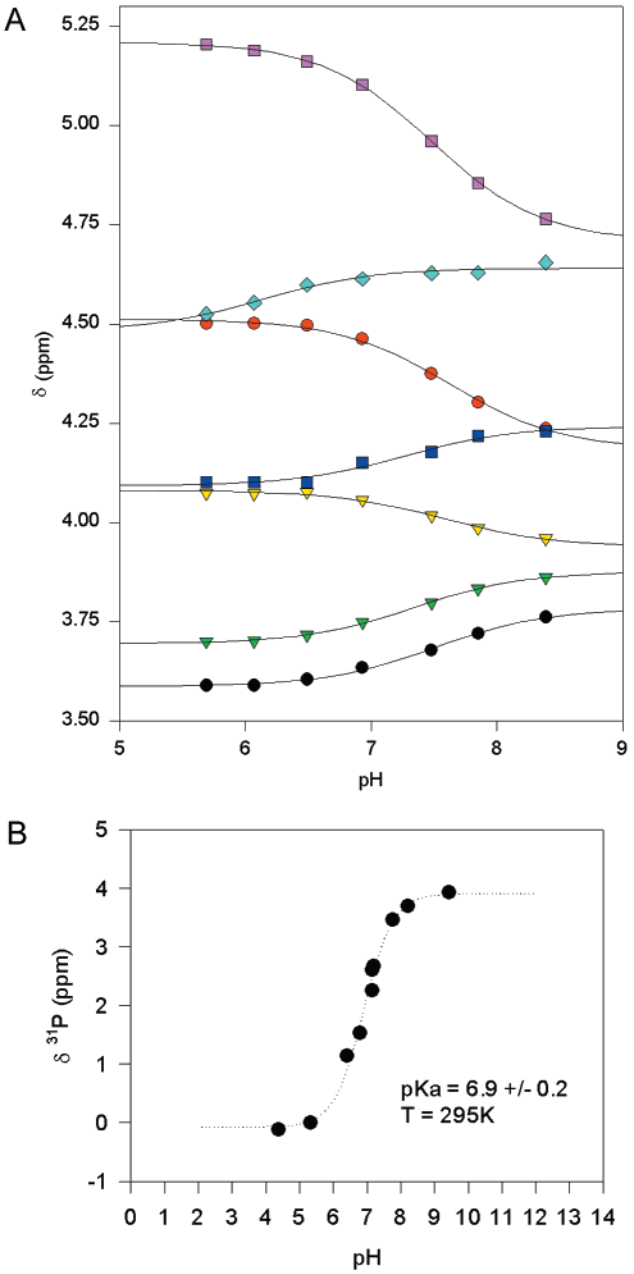

FIGURE 5: (A) pH-dependent chemical shifts of H_α proton resonances of pThr[45]-hirudin. The titration curves were fitted using the Henderson−Hasselbalch equation (solid lines). The symbols represent (■, pink) Gln[11], (▼, green) Gly[42]$_{\alpha1}$, (▼, yellow) Gly[42]$_{\alpha2}$, (■, blue) Glu[43], (●, black) Gly[44]$_{\alpha1}$, (●, red) Gly[44]$_{\alpha2}$, and (◆, light blue) Pro[46]. (B) Titration curve for the phosphate ester group attached to Thr[45]. Chemical shifts of the ^{31}P resonance were fitted according to the Henderson−Hasselbalch equation (dashed line). The resulting pK_a value is inserted in the diagram.

bond network in pThr[45]-hirudin at pH 8.0. However, the NMR fast-exchange regime, which prevails at pH 7.6−8.5, prevents direct NMR observations of the appropriate signals.

To test the hypothesis of a perturbed hydrogen bond network in pThr[45]-hirudin at pH values where the phosphate ester group is in the dianionic state, H/D exchange experiments were performed by MALDI-TOF mass spectrometry. In contrast to CD spectroscopy, where only the equilibrium content of secondary structure can be detected, hydrogen exchange experiments provide both structural and dynamic information (*13*, *14*, *20*).

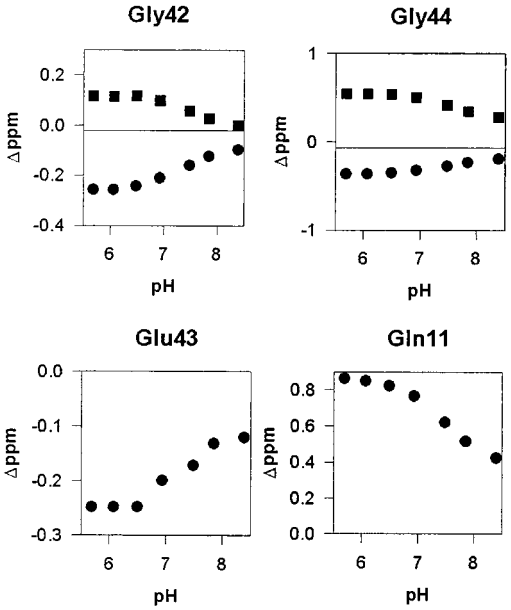

FIGURE 6: Chemical shift differences at various pHs of H_α protons referred to their random coil values. The chemical shift differences were calculated using the random coil values of Wishart et al. (*32*): the H_α protons of amino acids glycine (3.96 ppm), glutamic acid (4.35 ppm), and glutamine (4.34 ppm), respectively.

The formation of hydrogen bonds in peptides or proteins can slow the exchange of labile amide protons with deuterium atoms from the solvent. A temporary fission of these bonds (breathing) allows H/D exchange on a time scale where the rate constant is limited by breathing events. Under these conditions, the rate of deuterium incorporation is related to the lifetime of the hydrogen bonds. Molecules with identical structure and stability should thus exhibit identical deuterium incorporation kinetics. This method does not allow to detect the fraction of deuterium incorporated into groups with freely exchangeable hydrogens. Therefore, all observed deuterons are found to be present in secondary amide peptide moieties (−CONH−). The kinetics of deuterium incorporation is described by the equation

$$N_D(t) = N_{max} - \exp(-k_1 t) - \exp(-k_2 t) - \exp(-k_3 t) \ldots - \exp(-k_N t) \quad (1)$$

where $N_D(t)$ is the number of deuterated peptide bonds at time t, N_{max} is the total number of secondary amide peptide bonds, and k_1 to k_N represent the rate constants for the exchange of the individual protons. To simplify this multiexponential function, the peptidic protons exhibiting similar exchange rate constants were classified into four groups. Accordingly, A, B, C, and D are the numbers of protons that belong to the groups with either fast, medium, slow, or very slow exchange kinetics represented by the averaged exchange kinetic constants k_1, k_2, k_3, and k_4. Assuming that the groups with fast exchanging protons (group A) are always in the proton state due to the dead time of the experiments (10 s) and the very slowly exchanging protons (group D) do not undergo H/D exchange within the time period of the experiments (2 h), eq 1 simplifies to the equation

$$N_D(t) = N_{max} - A_C - B\exp(-k_2 t) - C\exp(-k_3 t) - D_C \quad (2)$$

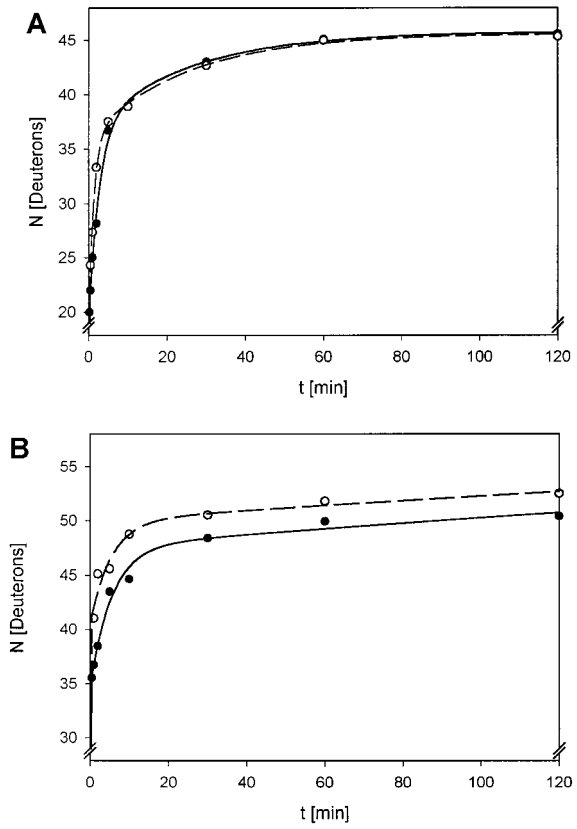

FIGURE 7: Time course of H/D exchange of peptide bond protons monitored by MALDI-TOF-MS. Exchange kinetics were recorded for hirudin (●) and pThr[45]-hirudin (○) at (A) pD 6.0 and (B) pD 8.0 (pD was corrected for isotopic effects). Each data point results from an individual exchange experiment. The deuterium content after exchange was averaged from three independent mass spectrometric measurements with an experimental error less than ±0.8 Da. Data were corrected for the residual 10% H_2O upon exchange experiment and for 5% back-exchange during sample preparation. Drawn lines represent the fits according to eq 2 (at pD 6.0) and eq 3 (at pD 8.0). Table 1 summarizes the exchange parameters used for the fits.

where $A_C = 0$ for $t > 0$ and $A_C = N_{max} - B - C - D_C$ for $t = 0$. In this equation A_C and D_C represent a constant number of protons. Curve fitting to eq 2 of the experimental data points depicted in Figure 7A (hirudin and pThr[45]-hirudin at pD 6.0) resulted in exchange parameters shown in Table 1. The rate constants k_2 and k_3 are similar for both hirudin and pThr[45]-hirudin. Furthermore, the partitioning between the four groups of the peptide bond protons in both proteins proved to be identical. Taken together, a significant influence on the hydrogen bond network of the monoanionic phosphate ester group can be excluded. However, the situation changes considering the dianionic state of the phosphate ester moiety. The proton number partitioning differs between hirudin and pThr[45]-hirudin at pH 8.0 (Figure 7B), and the proton numbers seen in the four groups are significantly different between pD 6.0 and pH 8.0. Due to the fast exchanging regime effective at pD 8.0 all protons exchange with the solvent on the time scale of 2 h. Under these assumptions eq 2 simplifies to

$$N_D(t) = N_{max} - A_C - B\exp(-k_2 t) - C\exp(-k_3 t) \quad (3)$$

The results of the analysis of the H/D exchange data of hirudin and pThr[45]-hirudin at pD 8.0 using eq 3 are summarized in Table 1. The kinetic constants k_2 and k_3 describing the exchange kinetics of the medium and slowly exchanging protons are similar in hirudin and pThr[45]-hirudin. In contrast, the sum of medium and slowly exchanging protons (groups *B* and *C*) is 26.4 in hirudin and 20.6 in pThr[45]-hirudin. The six "missing" protons emerge in the fraction of the fast exchanging protons. There are 40.4 protons belonging to group *A* in pThr[45]-hirudin and only 34.6 in hirudin. Obviously, the conversion of the phosphate ester moiety from the monoanionic to the dianionic form perturbs part of the hydrogen bond network. These changes occur solely in the direct proximity of the pThr−Pro bond, as indicated by the NMR spectroscopic experiments. Good candidates are the previously described $Gly^{42}H_N-Gly^{25}O$, $Gly^{25}H_N-Glu^{43}O^{\epsilon}$, $Asn^{12}H_N-Thr^{45}O$, and possibly $Thr^{45}H_N-Gly^{10}O$ hydrogen bonds, where the amide proton shifts show inflection points during the pH titration experiments.

Table 1: Calculated H/D Exchange Parameters of Hirudin and pThr[45]-Hirudin at pD 6.0 and pD 8.0

pD 8.0[a,c]	hirudin	pThr[45]-hirudin
A_C	34.6	40.4
B	13.0	9.5
C	13.4	11.1
k_2[d] (min^{-1})	2×10^{-1}	2×10^{-1}
k_3[d] (min^{-1})	2×10^{-3}	2×10^{-3}
pD 6.0[b,c]	**hirudin**	**pThr[45]-hirudin**
A_C	18.3	18.2
B	18.6	17.9
C	8.9	9.5
D_C	15.2	15.4
k_2[d] (min^{-1})	4×10^{-1}	8×10^{-1}
k_3[d] (min^{-1})	4×10^{-2}	4×10^{-2}

[a] Data were fitted according to eq 3. [b] Data were fitted according to eq 2. [c] The total number of secondary amide peptide bonds, $N_{max} = 61$ in hirudin and pThr[45]-hirudin, represents the sum of amide protons in groups $A + B + C$ at pD 8.0 and $A + B + C + D$ at pD 6.0, respectively. [d] Because of the low number of experimental data points the rate constants k_2 and k_3 are only approximate.

DISCUSSION

In this paper we could show that phosphorylation of Thr[45] of hirudin causes pH-dependent conformational changes. The pThr[45] flanking segment is sensitive to ionization of the phosphate ester group as probed by ^1H NMR and CD spectroscopy. The nature of the conformational changes could be elucidated by H/D exchange mass spectrometry, where data reveal a loss of hydrogen bond network dependent on ionization of pThr[45].

The chemical nature of the destabilizing effect of the phosphate ester group remains unknown. In addition to the second negative charge, which appears at pH 8, the dipole moment of the phosphate ester group is altered. Dipole−dipole interactions between the phosphate ester group and the amide proton of the phosphorylated residue are thought to represent "the driving force for the direct structural consequences of phosphorylation" (*29*). Electrostatic repulsion or attraction could therefore be one reason for the local structural changes described above. In Table 2 are given the distances from any charged oxygen atom of the phosphate group to the nearest charged groups (COO^- or N^+ of all arginine, lysine, and glutamic and aspartic acid residues),

Table 2: Distances of Charged or Dipolar Groups to the Nearest Oxygen Atom of the Phosphate Ester Group of pThr[45]

COO^-	distance (Å)	N^+	distance (Å)	dipole	distance (Å)
Glu^{43} Oϵ1	5.3	Lys^{27} Nζ	9.2	Gly^{44} C═O	4.4
Glu^{8} Oϵ1	9.7	Lys^{47} Nζ	12.2	Thr^{45} N−H	5.4
Asp^{5} Oδ1	20.5	Lys^{36} Nζ	25.9	Pro^{46} C═O	5.9
Glu^{35} Oϵ2	21.5				
Glu^{17} Oϵ2	22.5				
Asp^{33} Oδ2	23.6				

as calculated from a model of $pThr^{45}$-hirudin (InsightII, Biopolymer package). As can be seen, the only potential candidate for an efficient repulsion is Glu^{43} with a shortest possible distance between the nearest oxygen atoms of 5.3 Å. Supposing a maximum net oxygen charge of −1 and a dielectric constant of 40 (*24*) for the protein surface in a buffered aequeous solution, the free energy change ΔG would be approximately −2 kcal/mol. This is less than the binding energy (−4 kcal/mol) of a single hydrogen bond in water. Due to the distance criterion the charge-dipole interactions of the phosphate oxygens with polarized linkages such as the C═O, O−H, and N−H groups do not contribute much to ΔG (Table 2).

As the energy contribution of weak (rapidly exchanging) hydrogen bonds to the molecular stability is lower than the one from strong (slowly exchanging) hydrogen bonds found in β-sheets, α-helices, or turn elements, destabilization of $pThr^{45}$-hirudin at pH 8 is weak and results in partial unfolding in a limited volume of the molecule. Unfolding of small regions after site-directed covalent modifications of proteins seems to occur frequently but is difficult to detect. For example, uncoupling of the reaction rate of modification of the active site from depletion of catalytic activity serves as sensitive tool for local unfolding in enzymes (*10*). Here we provide a general tool for proteins, which are not subject to assays of activity.

The fact that switching from the monoanionic to the dianionic form of the phosphate group locally perturbs the ordered structure of a rather rigid protein leads to two further considerations. One could imagine a regulatory mechanism, governed by pH variations near to neutrality within cellular compartments, that would trigger catalysis by an enzyme or binding to a protein. Further, protein-mediated transport across membranes of different cellular compartments is sensitive to the binding rates of the interacting partners. The present results could then suggest an alternative model for many loading and unloading events of shuttle and carrier proteins. In the same way, the catalytic rate of specific enzymes could be triggered by the pH value or its gradient in the neighborhood of the mitochondrial membrane or various endosomes. In conclusion, this hypothesis opens a new perspective for evaluating phosphorylation events of proteins in the cell.

ACKNOWLEDGMENT

We thank Dr. R. Obermeier for a gift of hirudin and $pThr^{45}$-hirudin, A. Werner for a gift of PP2A, M. Seidel for technical assistance, and Prof. Dr. R. L. Schowen for carefully reading the manuscript.

REFERENCES

1. Barford, D. (1995) *Cur. Opin. Struct. Biol. 5*, 728−734.
2. Bornancin, F., and Parker, P. J. (1996) *Curr. Biol. 6*, 1114−1123.
3. Chen, G. J., Porter, M. D., Bristol, J. R., Fitzgibbon, M. J., and Pazhanisamy, S. (2000) *Biochemistry 39*, 2079−2087.
4. Coulot, M., Domon, B., Grossenbacher, H., Guenat, C., Maerki, W., Müller, D. R., and Richter, W. J. (1993) *J. Mol. Struct. 292*, 89−104.
5. Folkers, P. J., Clore, G. M., Driscoll, P. C., Dodt, J., Kohler, S., and Gronenborn, A. M. (1989) *Biochemistry 28*, 2601−2617.
6. Forest, K. T., Dunham, S. A., Koomey, M., and Tainer, J. A. (1999) *Mol. Microbiol. 31*, 743−52.
7. Hanks, S. K., and Hunter, T. (1995) *FASEB J. 9*, 576−96.
8. Haruyama, H., and Wüthrich, K. (1989) *Biochemistry 28*, 4301−12.
9. Haruyama, H., Qian, Y.-Q., and Wüthrich, K. (1989) *Biochemistry 28*, 4312−17.
10. Henning, L., Christner, C., Kipping, M., Schelbert, B., Rücknagel, K. P., Grabley, S., Küllertz, G., and Fischer, G. (1998) *Biochemistry 37*, 5953−5960.
11. Hurley, J. H., Dean, A. M., Sohl, J. L., Koshland, D. E., Jr., and Stroud, R. M. (1990) *J. Biol. Chem. 265*, 3599−3602.
12. Jia, Z. C. (1997) *Biochem. Cell Biol. 75*, 17−26.
13. Katta, V., and Chait, B. T. (1991) *Rapid Commun. Mass Spectrom. 5*, 214−217.
14. Katta, V., and Chait, B. T. (1993) *J. Am. Chem. Soc. 115*, 6317−6321.
15. Kern, D., Volkman, B. F., Luginbuhl, P., Nohaile, M. J., Kustu, S., and Wemmer, D. E. (1999) *Nature 402*, 894−898.
16. Kiriakis, J. M., and Avruch, J. (1994) in *Protein kinases* (Woodgett, J. R., Ed.) pp 85−132, URL Press, Oxford, New York, and Tokyo.
17. Lapko, V. N., Wells, T. A., and Song, P. S. (1996) *Biochemistry 35*, 6585−6594.
18. Li, M., Cornea, R. L., Autry, J. M., Jones, L. R., and Thomas, D. D. (1998) *Biochemistry 37*, 7869−7877.
19. Lin, K., Rath, V. L., Dai, S. C., Fletterick, R. J., and Hwang, P. K. (1996) *Science 273*, 1539−1541.
20. Miranker, A., Robinson, C. V., Radford, S. E., Aplin, R. T., and Dobson, C. M. (1993) *Science 262*, 896−900.
21. Mortishire-Smith, R. J., Pitzenberger, S. M., Burke, C. J., Middaugh, C. R., Garsky, V. M., and Johnson, R. G. (1995) *Biochemistry 34*, 7603−7613.
22. Piotto, M., Saudek, V., and Sklenar, J. (1992) *J. Biomol. NMR 2*, 661−665.
23. Pullen, K., Rajagopal, P., Branchini, B. R., Huffine, M. E., Reizer, J., Saier, M. H., Jr., Scholtz, J. M., and Klevit, R. E. (1995) *Protein Sci. 4*, 2478−2486.
24. Russell, A. J., Thomas, P. G., and Fersht, A. R. (1987) *J. Mol. Biol. 193*, 803−813.
25. Sayle, R. A., and Milner-White, E. J. (1995) *Trends Biochem. Sci. 20*, 374.
26. Schutkowski, M., Bernhardt, A., Zhou, X. Z., Shen, M. H., Reimer, U., Rahfeld, J. U., Lu, K. P., and Fischer, G. (1998) *Biochemistry 37*, 5566−5575.
27. Smith, D. L., Deng, Y. Z., and Zhang, Z. (1997) *J. Mass Spectrom. 32*, 135−146.
28. Szyperski, T., Guntert, P., Stone, S. R., and Wüthrich, K. (1992) *J. Mol. Biol. 228*, 1193−1205.
29. Tholey, A., Lindemann, A., Kinzel, V., and Reed, J. (1999) *Biophys. J. 76*, 76−87.
30. Wang, Q., Kline, A. D., and Wüthrich, K. (1987) *Biochemistry 26*, 6488−6493.
31. Zhou, X. Z., Kops, O., Werner, A., Shen, M., Lu., P.-J., Stoller, G., Küllertz, G., Stark, M., Fischer, G., and Lu, K. P. (2000) *Mol. Cell 6*, 873−883.
32. Wishart, D. S., Bigam, C. G., Halm, A., Hodges, R. S., and Sykes, B. D. (1995) *J. Biomol. NMR 5*, 67−81.
33. Gill, S. C., and von Hippel, P. H. (1989) *Anal. Biochem. 182*, 319−326.

BI010317R